

Electron spin dephasing in Mn-based II-VI diluted magnetic semiconductors

Z. Ben Cheikh, S. Cronenberger, M. Vladimirova, and D. Scalbert

Laboratoire Charles Coulomb, UMR 5221 CNRS-Université Montpellier 2, Place Eugene Bataillon, 34095 Montpellier Cedex 05, France

F. Perez

Institut des Nanosciences de Paris, UMR 7588 CNRS-Université Paris 6, Paris 75005, France

T. Wojtowicz

Institute of Physics, Polish Academy of Sciences, 02-668 Warsaw, Poland

(Received 9 September 2013; published 27 November 2013)

In various manganese-based II-VI diluted magnetic semiconductors and their quantum structures, the measured variations of electron spin dephasing time in an external magnetic field are conflicting with the most advanced spin relaxation theory based on quantum kinetic equations. We demonstrate, by time-resolved optical spin beat measurements performed on high-mobility *n*-doped CdMnTe quantum wells, that these contradictions are resolved if one takes into account the electron spin dephasing induced by laser heating of the manganese spins. We then provide a test of the spin relaxation theory in Mn-based quantum wells by a careful comparison with existing data, including our measurements. It turns out that the theory systematically underestimates the relaxation rates by a factor of 5.

DOI: [10.1103/PhysRevB.88.201306](https://doi.org/10.1103/PhysRevB.88.201306)

PACS number(s): 78.47.jm, 71.70.Jp, 78.20.Ls, 03.67.Bg

The research on electron spin relaxation processes in semiconductors has a long history,^{1,2} but is still very active as it is driven by eventual spintronics applications.^{3,4} While electron spin relaxation is reasonably well understood in non-magnetic semiconductors,⁵ a clear interpretation of electron spin relaxation in diluted magnetic semiconductors (DMSs) is still missing, even if spin-flip scattering of band electrons by the magnetic dopants is likely to be the dominant relaxation mechanism in these materials. This widely accepted picture is based on the fact that the electron spin relaxation observed in DMSs is much faster than in the nonmagnetic host semiconductors. Most of the reported results have been obtained by time-resolved Faraday and Kerr rotation experiments, in which the electron transverse spin relaxation time τ_e is deduced from the damping of the electron spin precession.⁶⁻¹² Typically it is observed that in low Mn concentration samples τ_e first decreases when a magnetic field is applied, reaches a minimum, and then increases again at higher field, while in high Mn concentration samples τ_e decreases steadily (see Fig. 1).

Fast relaxation is indeed expected from the *s-d* spin-flip rates calculated with Fermi's golden rule,^{13,14} or from a more elaborate theory based on quantum kinetic equations, which also predicts the evolution of the transverse and longitudinal relaxation times with the external magnetic field.¹⁵ However, the theory fails to reproduce the magnitude and the field dependence of τ_e , in various Mn-based quantum well (QW) structures,⁶⁻¹⁰ as well as in bulk CdMnTe^{11,12} (see Fig. 1). While the theory predicts an increase of the transverse spin relaxation time τ_e at low fields, then a decrease at higher fields,¹⁵ an opposite behavior is observed at least for low Mn concentrations. Theoretically, the nonmonotonous field dependence results from a competition between two contributions: The electron spin flips induced by the transverse components of the magnetic fluctuations, which dominate at small fields, and the

electron spin dephasing due to the longitudinal components of the magnetic fluctuations, which takes over at high fields. The same predictions follow from the phenomenological model proposed by Rönneburg *et al.*,¹¹ which assumes that the spin relaxation is induced by the fluctuations of the magnetization seen by the particle as it moves through the crystal. The effect of interface roughness on electron spin relaxation in QWs has been also considered theoretically, but has not received any experimental confirmation until now.¹⁶

In this Rapid Communication, we measure τ_e in CdMnTe QWs, by time-resolved Kerr rotation, for Mn concentrations lower than those reported earlier. This low doping regime favors longer spin relaxation times, and high quality samples suitable for comparison with theory. Then, by analyzing all available data, including those from literature, we show that the conflicting experimental and theoretical field dependencies of the electron spin dephasing time can be consistently understood if the inhomogeneous heating of the Mn spin system induced by the laser pulses is taken into account. This is shown to contribute to electron spin dephasing, and becomes the dominant dephasing mechanism at low Mn concentrations. We also checked that in Mn-based QWs the electron spin relaxation rate is inversely proportional to the QW width, and varies linearly with the effective Mn concentration times an integral, which defines by how much the electron feels the Mn spin fluctuations. Thereby, we demonstrate that the electron spin relaxation is dominated by the *s-d* spin-flip scattering for a wide range of Mn concentrations varying from $x = 0.0007$ to 0.30. However, the observed spin relaxation is found to be typically five times as fast as predicted by theory.

We purposely focus the experimental part of our study on CdMnTe QWs with low Mn concentrations, to better evidence the influence of thermal effects, and also because these are the best quality samples for which one can expect a meaningful comparison with theory. In addition, complications due to

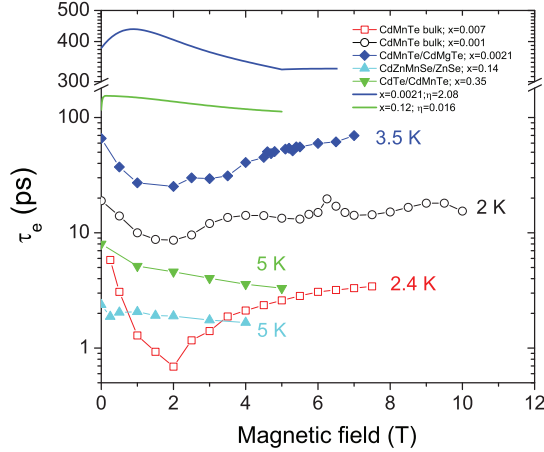


FIG. 1. (Color online) Selected data on spin dephasing time taken from literature and present work: (\square) Ref. 11, (\circ) Ref. 7, (\blacktriangledown) Ref. 12, (\blacktriangle) Ref. 8, (\blacklozenge) this work. The blue and green solid lines are calculated with the model of Ref. 15 with parameters corresponding to the experimental data (\blacklozenge and \blacktriangledown , respectively).

excitonic effects¹¹ are avoided by using n -doped QWs, in which the exciton is screened. The three studied samples contain a single modulation-doped CdMnTe QW of high mobility (see Table I). The Mn doping is uniform in samples A and B, while it consists of seven evenly spaced monolayers of Cd_{0.974}Mn_{0.026}Te in sample C. We performed ultrafast Kerr rotation experiments, in which spin polarized electrons are optically excited in the QW by a circularly polarized pump pulse, and then precess in a magnetic field applied parallel to the QW plane. The spin precession produces an oscillating Kerr signal detected by a delayed probe pulse. In our experimental setup the pump and probe pulses are spectrally filtered with two $4f$ zero-dispersion lines, and the laser spot size on the sample is $\sim 100 \mu\text{m}$.

Figure 2(a) displays the Fourier spectra of the Kerr signal for a series of magnetic field intensities. The observed line is associated with electron spin precession in the CdMnTe QW. The Zeeman effect and the s - d exchange interaction proportional to the Mn magnetization compete to produce the observed nonmonotonous frequency shift with magnetic field. The line splits into two components around 5 T, revealing an avoided crossing between the electron and Mn spin-flip excitations. It corresponds to the onset of a correlated electron-Mn spin precession due to dynamic exchange coupling,

TABLE I. Main characteristics of the studied QWs: n_e is the electron concentration, x is the effective Mn concentration, W is the QW width, η is the overlap integral defined in the text, μ is the mobility, and g_e is the electron g factor.

Samples	A	B	C
n_e (cm ⁻²)	3.4×10^{11}	1.9×10^{11}	4.3×10^{11}
x	0.0021	0.0007	0.0028
W (nm)	30	30	21
η	2.08	1.77	1.62
μ (cm ² /V/s)	110 000	146 000	170 000
g_e	-1.72	-1.68	-1.71

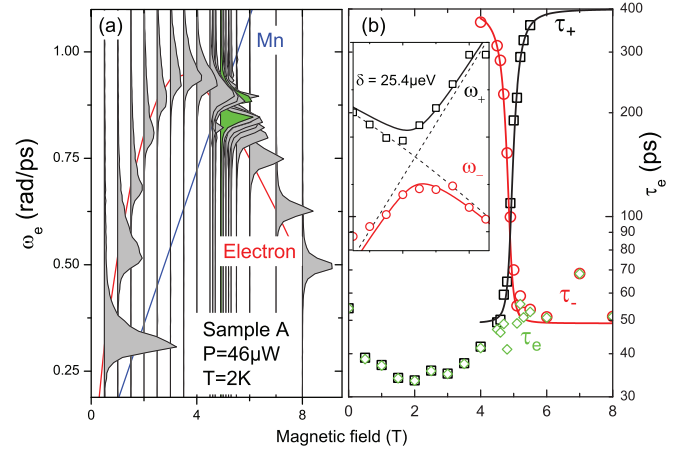


FIG. 2. (Color online) Left panel: Evolution of the Fourier power spectra of the time-resolved Kerr rotation as a function of magnetic field, in conditions where the electronlike and Mn-like modes cross each other. The spectrum corresponding to the anticrossing is highlighted in green. Right panel: Frequencies and relaxation times of the two mixed modes ω_{\pm} in the region of the anticrossing. The green diamonds represent the electron spin relaxation time corrected from the effect of dynamic coupling with Mn²⁺ spins (see text).

and two coupled modes of electron and Mn precession ω_{\pm} emerge.^{10,17,18} As can be seen in Fig. 2(b), the two coupled modes exhibit rapidly varying relaxation times τ_{\pm} in the crossing region, due to the varying admixture of electron and Mn spin excitations in the coupled modes. To get rid of the effect of this admixture in the electron spin relaxation time, which is not included in the theoretical models,¹⁹ we extract the electron spin relaxation τ_e from the usual equation for coupled oscillators $(\tilde{\omega}_{\pm} - \tilde{\omega}_e)(\tilde{\omega}_{\pm} - \tilde{\omega}_{\text{Mn}}) = \Omega^2$, where $\tilde{\omega}_e$ and $\tilde{\omega}_{\text{Mn}}$ are the complex precession frequencies of the electron and Mn, respectively, and Ω is the coupling parameter.^{18,20} As $\tau_{\text{Mn}} \gg \tau_e$ we assume that ω_{Mn} is real, and get $\tau_e^{-1} = \text{Im}[\tilde{\omega}_{\pm} - \frac{\Omega^2}{(\tilde{\omega}_{\pm} - \omega_{\text{Mn}})}]$. As can be seen in Fig. 2(b), the resulting τ_e (green diamonds) is not far from a mere extrapolation of the data, and smoothly varies in the anticrossing region.²¹

Important parameters of the experiment, such as the electron g factor g_e , the effective Mn²⁺ concentration x , and the effective Mn²⁺ spin temperature T_{eff} , can be deduced from the variation of ω_e with field (see Table I). Indeed, ω_e contains two contributions: the Zeeman effect, and the s - d exchange interaction. It can be fitted using $\hbar\omega_e(B, T_{\text{eff}}) = g_e\mu_B B + \alpha M_z / (g_{\text{Mn}}\mu_B)$ [solid lines in Figs. 3(a) and 3(b)], where g_{Mn} is the Mn²⁺ g factors, μ_B is the Bohr magneton, α denotes the exchange coupling constant between Mn²⁺ ions and itinerant electrons, and M_z is the magnetization of the Mn²⁺ ions described by a Brillouin function.²² A salient feature of ω_e is its marked dependence on laser power at 2 K, which disappears at 12 K [Fig. 3(a)]. As a corollary, the nonmonotonous field dependence of τ_e observed at 2 K almost disappears at 12 K [Fig. 3(c)]. This strongly suggests that the variations of τ_e observed at 2 K are a consequence of thermal effects. Indeed, one expects a strong reduction of laser heating upon raising the lattice temperature due to a rapid increase of specific heat. Therefore, we interpret the nonmonotonous field dependence of τ_e as a consequence of the inhomogeneous

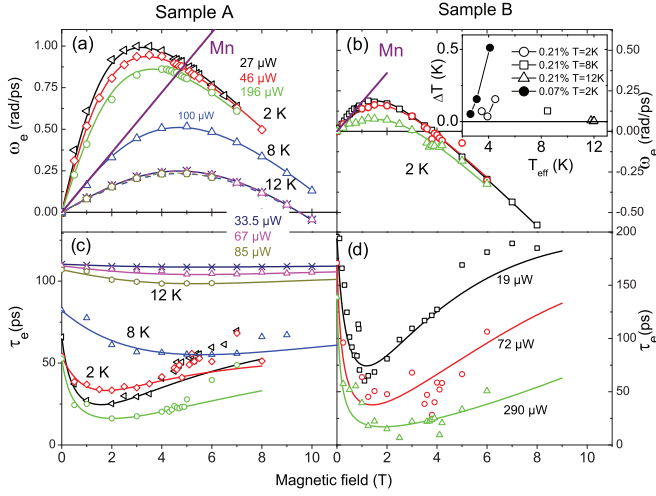


FIG. 3. (Color online) Magnetic field dependencies of electron precession frequency and spin relaxation time measured in samples A (left panel) and B (right panel), for different powers and helium bath temperatures. Solid lines in (a) and (b) are fits to ω_e with a linear Zeeman term plus a Brillouin function. Solid lines in (c) and (d) are fits to τ_e with the model of inhomogeneous heating described in the text. The inset shows how the variance of the temperature distribution ΔT and the effective Mn^{2+} temperature T_{eff} , deduced from the fits, correlate when the laser power changes.

distribution of temperatures within the laser spot profile. For simplicity we assume a Gaussian distribution of temperatures T_{eff} with variance ΔT , resulting in a Gaussian distribution of magnetizations with variance

$$\Delta M_z = \frac{N_0 x (g_{\text{Mn}} \mu_B S)^2}{k_B T_{\text{eff}}^2} B'_S \left(\frac{g_{\text{Mn}} \mu_B S B}{k_B T_{\text{eff}}} \right) B \Delta T. \quad (1)$$

N_0 is the density of unit cells of the host lattice, $S = 5/2$, and B'_S is the first derivative of the normalized Brillouin function. As ω_e strongly depends on magnetization, electron spins located at different positions within the spot will dephase, so that the total dephasing rate in presence of inhomogeneous heating will be

$$\frac{1}{\tau_e^*(B, T_{\text{eff}})} = \frac{1}{\tau_e(B, T_{\text{eff}})} + \frac{1}{\sqrt{2}} \frac{\alpha \Delta M_z}{\hbar g_{\text{Mn}} \mu_B}. \quad (2)$$

For a quantitative comparison with experimental data we assume $\tau_e(B, T_{\text{eff}}) = \tau_e(0, T_{\text{eff}})$.²³ Figures 3(c) and 3(d) show that this simple model reproduces quite well the data for different samples, temperatures, and laser powers. The minimum of τ_e^* is reached at a field B_m increasing with temperature, also in agreement with the model, according to which $B_m/T_{\text{eff}} \simeq 0.46$ T/K. The inset of Fig. 3 shows that ΔT and T_{eff} are correlated when the laser power changes, and that ΔT decreases either upon increasing x or T . This is a direct consequence of the increase of the magnetic or lattice specific heat, respectively. The model also explains the minimum of τ_e observed in bulk samples around 2 T (see Fig. 1), while for large x (up and down triangles) no thermal effects are in order due to the large magnetic specific heat.²⁴ For these large concentrations a small decrease of the relaxation time with rising magnetic field is observed. This is most probably related to the increase of the magnetic fluctuations along the

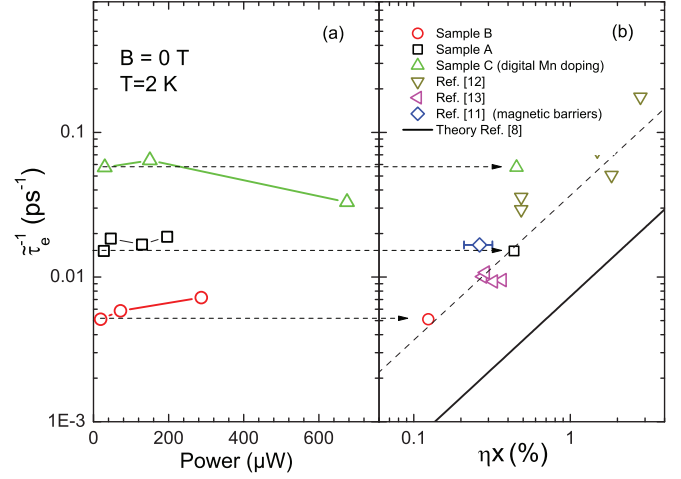


FIG. 4. (Color online) Left panel: Normalized relaxation rates (see text) vs power for the three studied samples. Right panel: Experimental (solid symbols), including data taken from literature, and theoretical (solid line) normalized relaxation rates. The dashed line corresponds to the theoretical relaxation rates multiplied by a factor of 5.

external field, which arise due to random spatial distribution of the magnetic ions.^{11,15}

As the spin dephasing induced by the inhomogeneous heating disappears at zero field, or at high temperatures, only in these conditions can a meaningful comparison with theory be attempted. Here we focus on zero-field spin relaxation, which is not affected by other possible spin dephasing mechanisms.^{16,25} From the theory¹⁵

$$\tau_e^{-1}(0, T) = \eta \frac{N_0 x S(S+1) \alpha^2 m_e}{3 \hbar^3 W}, \quad (3)$$

where m_e is the electron effective mass, $\eta = W \int_{-\infty}^{+\infty} \frac{n_m(z)}{n_m} |\psi(z)|^4 dz$, $\psi(z)$ is the perpendicular to the plane electron envelope function, and n_m and $n_m(z)$ are the average and local Mn^{2+} concentrations, respectively.

In order to compare the relaxation rates measured on QWs with widely different widths W , and overlap integrals η , we plot the normalized relaxation rates defined as $\tilde{\tau}_e^{-1} = \frac{W}{W_{\text{ref}}} \tau_e^{-1}$ against the product ηx [Fig. 4(b)]. We choose as a reference $W_{\text{ref}} = 30$ nm, corresponding to the QW width of samples A and B. We estimate the intrinsic $\tilde{\tau}_e^{-1}$ by extrapolating to zero laser power the measured relaxation rates [Fig. 4(a)], and calculate η for each sample, by solving self-consistently the coupled Schrödinger-Poisson equations. The obtained values of $\tilde{\tau}_e^{-1}$ are then compared to data adapted from literature [Fig. 4(b)]. Remarkably, the normalized relaxation rates closely follow the linear dependence predicted by the theory, for a large range of Mn^{2+} concentrations, QW widths, carrier doping and mobility, and integrals η , including the nonmagnetic QW with magnetic barriers $\text{Cd}_{0.7}\text{Mn}_{0.3}\text{Te}$ studied in Ref. 8. As the Mn profile at the interface is not known for this sample, we estimate ηx for two extreme cases. First, we assume a steplike profile with effective concentration in the barrier $x = 0.12$,²⁶ deduced from the measured splitting of the conduction band, and $\eta = 0.016$ calculated assuming a 60% conduction band offset.²⁷ Second, we assume a delta doping of Mn at the interface producing identical electron spin

splitting. These two extreme cases yield the error bar on ηx , as shown in Fig. 4(b). The linear variation of $\tilde{\tau}_e^{-1}$ with ηx clearly confirms that the spin relaxation in these QWs is governed by the exchange interaction between itinerant electrons and Mn^{2+} ions. The digital sample exhibits slightly faster spin relaxation than other QWs, possibly indicating the influence of a nonrandom alloy substitution on spin relaxation.

In summary, we have shown that the electron spin dephasing time deduced from optical spin beat measurements is strongly affected by laser heating of the Mn spin subsystem, even at the lowest experimentally accessible laser powers. This makes experimental checks of electron spin relaxation theory tricky in DMSs. Laser heating in these systems manifests itself as an anomalous field dependence of the electron spin dephasing time, which disappears as the Mn-lattice specific heat increases upon raising either the Mn concentration or the lattice temperature. This anomalous field dependence can be understood in terms of electron spin dephasing in the inhomogeneously heated magnetization of the Mn^{2+} ions. This

allowed us to identify the conditions in which a meaningful comparison with theory can be attempted, such as in zero field.

We thus checked that the zero-field electron spin relaxation time is governed by the Mn^{2+} concentration, the QW width, and η , an integral depending on the overlap between electron and magnetic ion wave functions, in full agreement with electron spin relaxation theory. Thereby, we confirmed that the electron spin relaxation is dominated by the s - d exchange interaction, for a wide range of Mn^{2+} concentrations between $x = 0.0007$ and 0.3 . However, the spin relaxation is found to be typically five times faster than predicted, even in very clean samples with low magnetic disorder.

D.S. acknowledges discussions with Y. G. Semenov. We gratefully acknowledge financial support by the Agence Nationale de la Recherche (Contract No. ANR-07-BLAN-0252), and by the FP7 EU ITN INDEX (289968). The research in Poland was partially supported by the National Science Centre (Poland) under the Grant No. DEC-2012/06/A/ST3/00247.

¹*Optical Orientation*, edited by F. Meier and B. Zakharchenya, Modern Problems in Condensed Matter Science Series Vol. 8 (North-Holland, Amsterdam, 1984).

²*Spin Physics in Semiconductors*, edited by M. Dyakonov (Springer, Berlin, 2008).

³S. A. Wolf, D. D. Awschalom, R. A. Buhrman, J. M. Daughton, S. von Molnár, M. L. Roukes, A. Y. Chtchelkanova, and D. M. Treger, *Science* **294**, 1488 (2001).

⁴D. Awschalom and M. Flatté, *Nat. Phys.* **3**, 153 (2007).

⁵K. V. Kavokin, *Semicond. Sci. Technol.* **23**, 114009 (2008).

⁶S. A. Crooker, J. J. Baumberg, F. Flack, N. Samarth, and D. D. Awschalom, *Phys. Rev. Lett.* **77**, 2814 (1996).

⁷S. A. Crooker, D. D. Awschalom, J. J. Baumberg, F. Flack, and N. Samarth, *Phys. Rev. B* **56**, 7574 (1997).

⁸R. Akimoto, K. Ando, F. Sasaki, S. Kobayashi, and T. Tani, *Phys. Rev. B* **57**, 7208 (1998).

⁹C. Camilleri, F. Teppe, D. Scalbert, Y. G. Semenov, M. Nawrocki, M. Dyakonov, J. Cibert, S. Tatarenko, and T. Wojtowicz, *Phys. Rev. B* **64**, 085331 (2001).

¹⁰P. Barate, S. Cronenberger, M. Vladimirova, D. Scalbert, F. Perez, J. Gomez, B. Jusserand, H. Boukari, D. Ferrand, H. Mariette *et al.*, *Phys. Rev. B* **82**, 075306 (2010).

¹¹K. E. Rönnburg, E. Mohler, H. G. Roskos, K. Ortner, C. R. Becker, and L. W. Molenkamp, *Phys. Rev. Lett.* **96**, 117203 (2006).

¹²S. Cronenberger, M. Vladimirova, S. V. Andreev, M. B. Lifshits, and D. Scalbert, *Phys. Rev. Lett.* **110**, 077403 (2013).

¹³G. Bastard and R. Ferreira, *Surf. Sci.* **267**, 335 (1992).

¹⁴Y. G. Semenov and F. V. Kirichenko, *Semicond. Sci. Technol.* **11**, 1268 (1996).

¹⁵Y. G. Semenov, *Phys. Rev. B* **67**, 115319 (2003).

¹⁶P. M. Shmakov, A. P. Dmitriev, and V. Y. Kachorovskii, *Phys. Rev. B* **80**, 193205 (2009).

¹⁷F. J. Teran, M. Potemski, D. K. Maude, D. Plantier, A. K. Hassan, A. Sachrajda, Z. Wilamowski, J. Jaroszynski, T. Wojtowicz, and G. Karczewski, *Phys. Rev. Lett.* **91**, 077201 (2003).

¹⁸M. Vladimirova, S. Cronenberger, P. Barate, D. Scalbert, F. J. Teran, and A. P. Dmitriev, *Phys. Rev. B* **78**, 081305 (2008).

¹⁹Existing theories of electron spin relaxation in DMSs consider the magnetic subsystem as a spin bath at thermal equilibrium, in which the spin coherence is rapidly lost (see, e.g., Ref. 15). This assumption relies on the existence of non-spin-conserving interactions in the magnetic subsystem, which contains many more spins than the free electrons subsystem. It is likely to be valid in general, except when the electron and Mn spin-flip excitations cross each other. In such a situation the spin coherence oscillates back and forth between the two spin systems, before spin coherence is lost.

²⁰J. König and A. H. MacDonald, *Phys. Rev. Lett.* **91**, 077202 (2003).

²¹We note that a correlated spin precession is not expected as the field $B \rightarrow 0$, because in this case the dynamic exchange coupling vanishes.

²²J. A. Gaj, R. Planel, and G. Fishman, *Solid State Commun.* **29**, 435 (1979).

²³Assuming instead that τ_e smoothly varies with magnetic field, as expected from theory, does not change our conclusions.

²⁴R. R. Galazka, S. Nagata, and P. H. Keesom, *Phys. Rev. B* **22**, 3344 (1980).

²⁵R. Bratschitsch, Z. Chen, S. T. Cundiff, E. A. Zhukov, D. R. Yakovlev, M. Bayer, G. Karczewski, T. Wojtowicz, and J. Kossut, *Appl. Phys. Lett.* **89**, 221113 (2006).

²⁶This large value of x results from magnetic dilution at the QW interfaces (Ref. 28).

²⁷J. Siviniant, F. V. Kyrychenko, Y. G. Semenov, D. Coquillat, D. Scalbert, and J. P. Lascaray, *Phys. Rev. B* **59**, 10276 (1999).

²⁸J. A. Gaj, W. Grieshaber, C. Bodin-Deshayes, J. Cibert, G. Feuillet, Y. Merle d'Aubigné, and A. Wasiela, *Phys. Rev. B* **50**, 5512 (1994).